TRAVAUX, Proceedings of the 3rd International Congress of ICSOBA , Nice, 17 - 21 September 1973

Investigation of the reaction kinetics and material transport in the Bayer process using radioisotopes

E. BUJDOSÓ and M. ORBÁN

Studies carried out in various phases of the Bayer process by means of radioisotope techniques are discussed. These studies include material flow and mixing measurements in continuous equipment, autoclaving and aluminate liquor decomposition tanks in series, settling equipment, as well as investigations of reaction kinetics in red mud wash, causticization and aluminate liquor decomposition operations.

1. INTRODUCTION

Radioisotope techniques have opened up new prospects in industrial research in general and in laboratory and industrial-scale studies within the alumina industry in particular. The first use of the tracer technique in alumina plants was reported by Japanese researchers [1]. This was soon followed by similar work in Hungary [2] and in the Federal Republic Germany [3]. This has been continued since on an increasingly broad basis. We wish to refer here to the excellent review by Winkhaus [4] on the utilization of radioisotopes in the alumina industry published recently by Eurisotop.

Research in this field may be grouped around four main subjects:

(1) Studies on mass flow and mixing in alumina plant equipment. Such measurements were performed in autoclaves in series, [1], [2], [4-9], tube reactors [3], [4], [9], settlers [1], [4], [8], [10-12], liquor evaporators [13], aluminate liquor decomposition tanks in series [14], [15] and calcining furnaces [1].

(2) Studies on the reaction kinetics of alumina plant processes, using labelled atoms [16-19], organic compounds [20] and activation analysis [21].

(3) Development of neutron activation methods and apparatus for the determination of macro- and microconstituents in bauxite [22-27] red mud [27] and alumina [28].

(4) Methods based on the absorption of gamma radiation for measuring the density [4], settling [19], [29] and particle size distribution [30] of slurries in alumina plants.

Devices using radioisotopes for level indication in alumina plants — although they do not belong to the scope of research — should also be mentioned.

Such devices contribute to the automation of alumina plants.

In this paper we wish to report the most recent results obtained with radioisotope methods in the Institute for Non-Ferrous Metals. The results will be discussed in the order of operations in the Bayer process.

2. BAUXITE DIGESTION

The ideal case of material flow in continuous digesting equipment is the plug flow. This can be fully effectuated in tube reactors only. In autoclaves in series, the residence time and distribution function of the material depends on the number of autoclaves, on their volume and on the extent of agitation. The suitability of various types of autoclaves in series was studied by measuring the activity distribution functions of radioisotopes fed to the system in pulses. The data obtained in these measurements served as a basis for developing a simple mathematical model that yields a good approach of the distribution functions of actual mixing conditions.

The distribution functions of perfect mixing in tank series are described by non-complete gamma functions [31]. By taking the mixing efficiency into account, the real distribution functions can be derived as can be seen in Fig. 1 [32]. With decreasing mixing efficiency, the deviation between the theoretical case and the real distribution functions will become larger. The knowledge of the real distribution functions will not only allow optimation of existing autoclaves in series, but also the pre-determination of the effect of agitation to be utilized in design work. Our results have largely contributed to the successful operation of Hungarian digesting series.

PERFECT MIXING: $F_i(\Theta) = \Gamma_i(\Theta)$

INCOMPLETE MIXING: $F_i(\Theta) = \Gamma_i\left(\frac{\Theta}{\eta_i}\right)$

Γ_i - INCOMPLETE GAMMA FUNCTIONS

$\Theta = \frac{t}{\tau}$, τ - TH. MEAN RES. TIME

η_i - MIXING EFFICIENCY

Fig. 1. — Residence time distribution functions

3. SETTLING OF RED MUD

The physicochemical and chemical properties of bauxite and the phase composition and morphology of red mud as well as the applied settling agent unequivocally define the settling, wash and filtering properties of the red mud. It is one of the research objectives of our Institute to disclose these relationships. In view of increased requirements, the measurement of the mud level sinking rate is not satisfactory for the study of red mud settling and thickening properties. Therefore, we developed an apparatus based on the absorption of gamma-rays (Fig. 2). The ^{241} Am source and the detector move up and down along the thermostated settling tube. The intensity of gamma-rays is recorded by an X-Y recorder. A photograph of the apparatus is shown in Fig. 3.

A recorded graph obtained in settling measurements of a red mud from Halimba bauxite is presented in Fig. 4 [33]. The figure may be interpreted as follows: in the settling range of the slurry, the solids concentration remains constant and is identical with the initial value. In the thickening range, the solids concentration starts to increase immediately after the beginning of the settling operation, in the lower part of the tube. In the followings, the course of thickening may be conceived as the upward propagation of the concentration values produced in the settled slurry. This, however, proceeds only up to

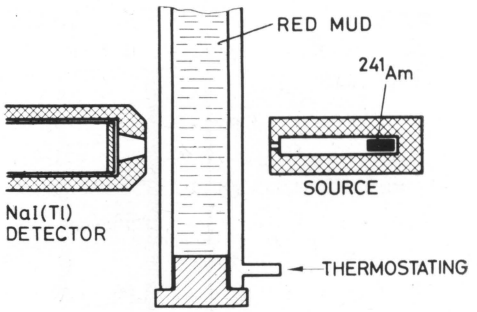

Fig. 2. — Scheme of the sedimentation apparatus

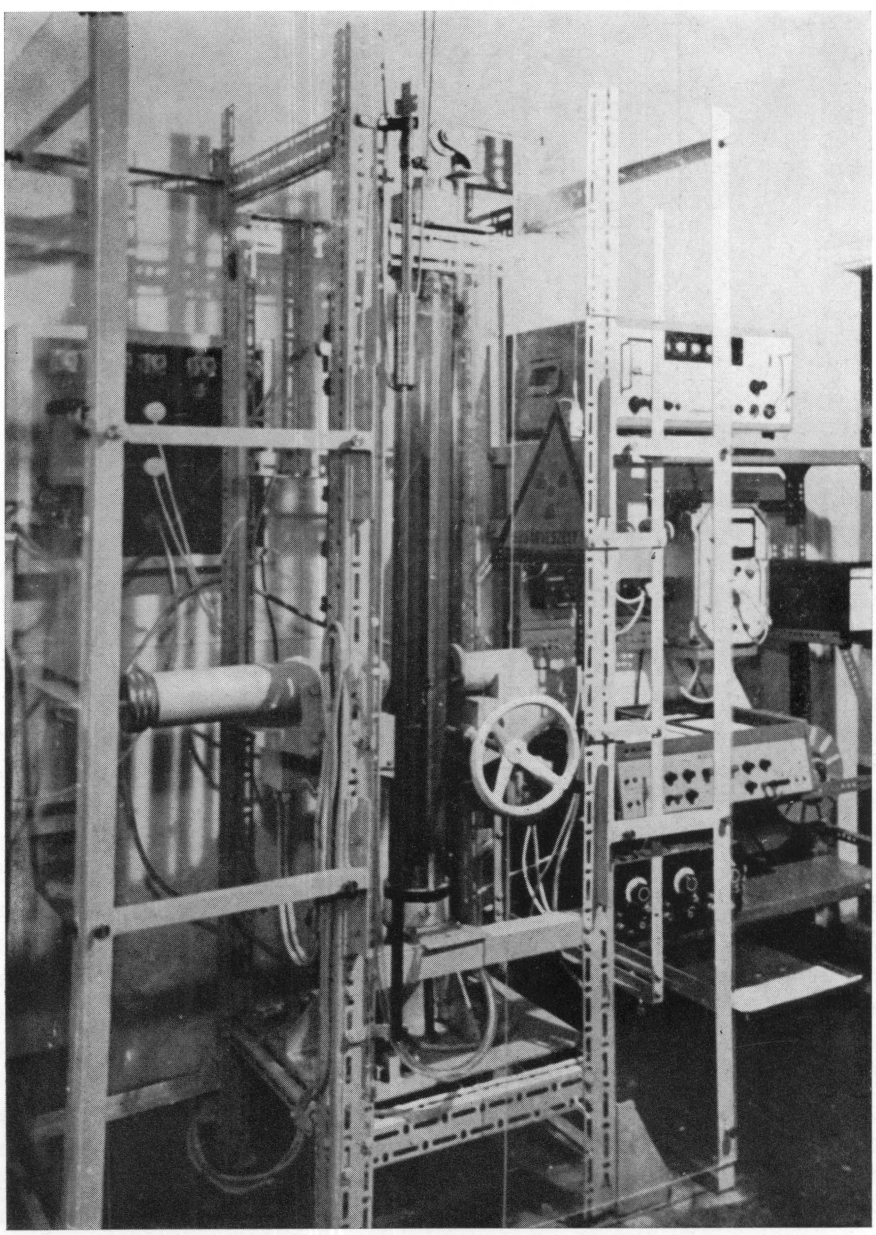

Fig. 3

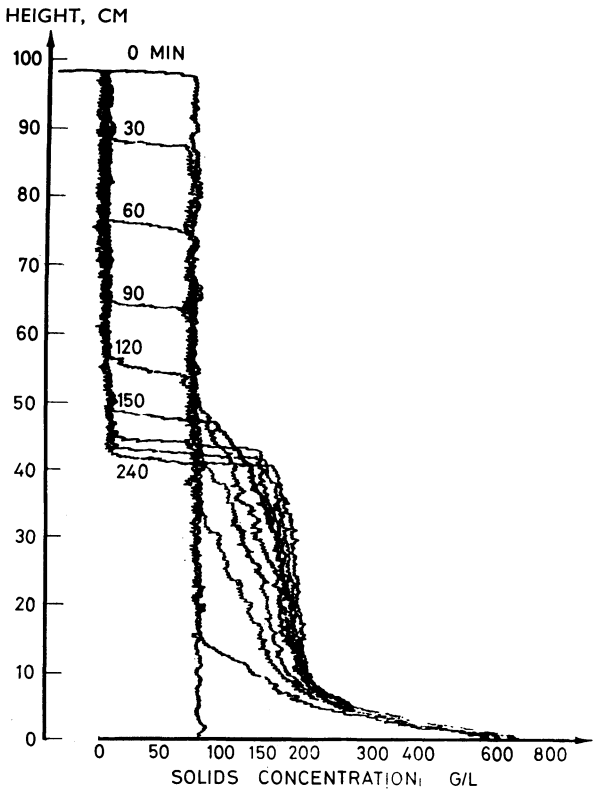

Fig. 4. — Density profiles of settling

a defined concentration limit. At the meeting of the thickening and settling zone, the major part of the slurry will assume this limiting concentration (in the given case ~ 180 g/litre). In the lower part of the tube, concentration distribution is exponential (i.e. a straight line in the logarithmic diagram). After a certain period, when equilibrium is attained, this will be characteristic for the total thickened zone. Settling agents affect the settling rate, and later — when the settling zone ceases — they affect the value of the concentration limit and the length of the zone with this concentration.

Under dynamic conditions, in industrial equipment, settling proceeds in a different manner. Radioisotope tracer studies were applied to disclose the relationship between the two processes. These will be illustrated by the following sample.

The flow of the solid and liquid phases was studied simultaneously by a double tracer technique using ^{59}Fe for the solid phase and ^{32}P for the liquid phase. The experiment was carried out in a single-chamber thickener (diam. 35 m) shown in Fig. 5. In the activity distribution of the clear liquor leaving through the overflow, two exponential components can be distinguished (Fig. 6). The fast component indicates the mixing process between the liquor phase fed in with the red mud, and the liquor of the settling zone in the thickener. The slow component demonstrates the exit of the labelled liquor through the thickening zone, the latter acting — as it were — as a filter. The filtration rate successively decreases as the zone becomes more and more compact, and finally the linear velocity of the upward flow of the liquor will be less than the downward velocity of the slurry brought about by outflow. Hence, this liquor will remain enclosed between the solid particles and will leave together with them. In the outflow of slurry, a time lag will appear between the volumes of simultaneously entering solid and liquid phases, due to the upward diffusion of the liquor. This time lag can be determined by using the distribution function presented in Fig. 7.

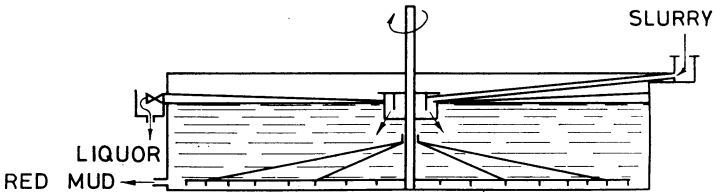

Fig. 5. — Scheme of a dorr-type thickener

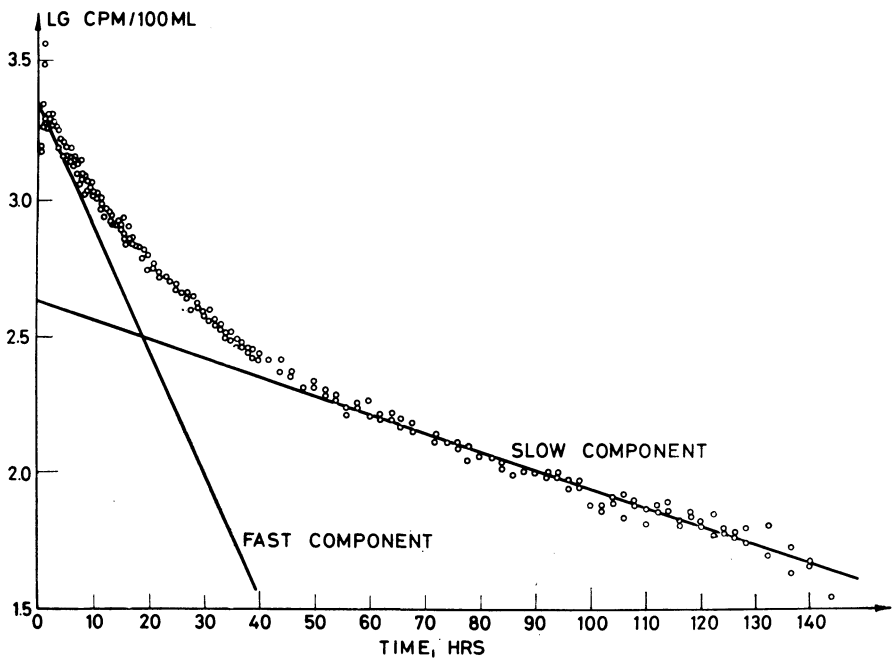

Fig. 6. — Residence time of clear liquor

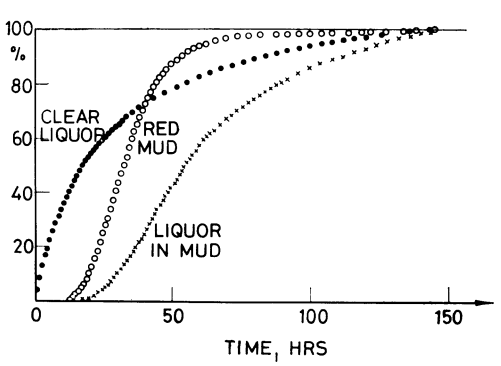

Fig. 7. — Distribution functions of a thickener

4. RED MUD WASH

The objective of red mud washing is to reduce the caustic soda losses due partly to the liquor enclosed between the red mud particles and partly to the sodium compounds formed as a result of the silica and titanium content of bauxite. To enable high-accuracy and high-sensitivity determinations of Na_2O, the washing experiments were carried with ^{24}Na tracer added to the digesting liquor. Hence, the radioactive atoms were incorporated together with the inactive sodium atoms, at identical ratio, into the system formed, i.e. into the sodium aluminium hydrosilicates and sodium titanates. Sodium aluminium hydrosilicates are characterized by the formula $3(Na_2O \cdot Al_2O_3 \cdot 2SiO_2)Na_2X \cdot nH_2O$ where X stands for any contamination present in the aluminate liquor. The sodium-containing phases formed from the anatase content of the bauxite correspond to the formulae $Na_2Ti_2O_5$ (10%), $Na_2Ti_3O_7$ (20%) and $Na_2Ti_3O_7 \cdot 2H_2O$ (20%).

In the multistage washing experiments of red mud samples combined with centrifuge separation, two sections have been distinguished in the change of Na_2O concentration of the wash water (Fig. 8). The rapidly decreasing exponential part of the curve corresponds to the dilution of the liquor adhering to the red mud particles, while the slow decrease represents the dissolution of the sodium-containing compounds. The slope of the rapid stage is mainly affected by the extent of dilution, whereas the slope of the slow stage depends on the residence time in the individual washing stages.

The latter process has been studied extensively by means of sodium aluminium hydrosilicate and sodium titanate model substances labelled with ^{24}Na. The adhering liquor was removed by a three-stage rapid wash. Subsequently dissolution experiments were performed at 90 °C with distilled water, at varying solids concentrations.

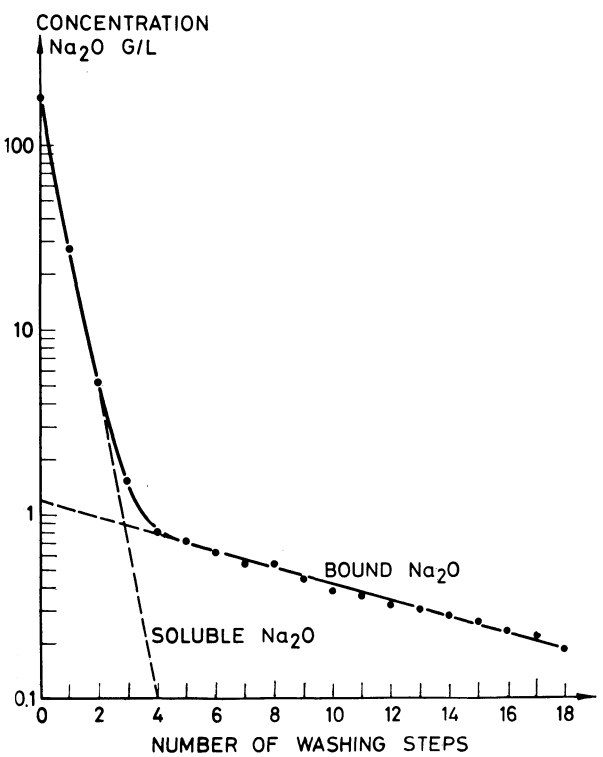

Fig. 8. — Stepwise washing of red mud

By way of example, Fig. 9 demonstrates the concentration changes of Na_2O, Al_2O_3 and SiO_2 for the case of a hydroxide-sodalite solution. After an initial rapid increase in the concentration of all three constituents, corresponding approximately to the stoichiome-

tric composition, Al_2O_3 and SiO_2 concentrations decrease, while Na_2O concentration — though at a reduced rate — continues to increase. Similar observations were made with chloride and carbonate sodalite and with cancrinite, but the concentration values in the solutions were different. X-ray diffraction studies of the solid phase demonstrated that in the course of dissolution, structural transformations and the formation of aluminium silicate hydrate [$Al_2Si_2O_5(OH)_4 \cdot 2H_2O$] proceed.

Although the character of the dissolution curves is identical, the actual Na_2O concentration of the solution also depends on the solid matter concentration of the model substances. This dependence and the solubility sequence of the model substances is presented in Fig. 10. The amount of dissolved Na_2O is related to the initial Na_2O content of the solid phase and to the rapid initial phase of the dissolution process. The figure indicates that OH-sodalite is the most readily soluble and cancrinite the most slowly soluble [34] among the compounds in question. Thus the study led to the conclusion that in order to reduce caustic soda losses, technology should be modified so as to lead to the formation of sodium compounds readily removed by washing.

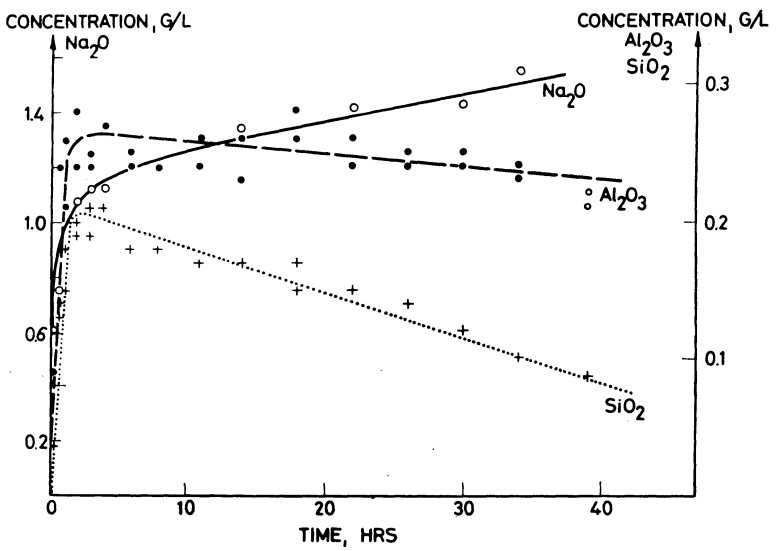

Fig. 9. — Dissolution curves of OH-sodalite

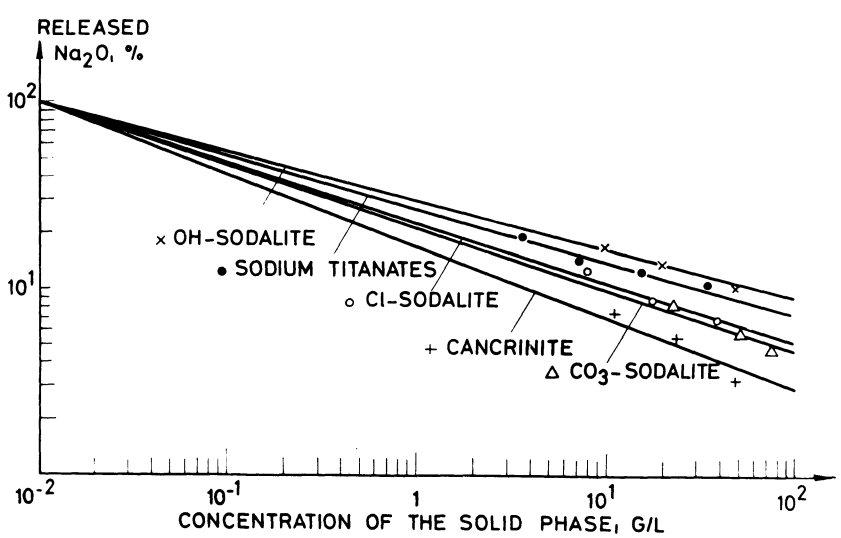

Fig. 10. — Dissolution of model substances

5. DECOMPOSTION OF ALUMINATE LIQUORS

The purity of alumina hydrate obtained in the decomposition operation is substantially affected by impurities present in the liquor. Measurements of the activity of radioactive tracers added to the liquor led to the conclusion that all contaminants that are present in the aluminate liquor in the form of OH-containing anions will be incorporated — presumably by isomorphous substitution — into the alumina hydrate, while contaminants not containing OH-groups are not significant as to the purity of the hydrate, if satisfactory wash is provided [17], [18].

Particular attention was paid to the behaviour of dissolved and suspended iron compounds in the course of the decomposition operation [21]. The bauxite samples were activated in a nuclear reactor, ensuring that the various iron minerals contained in the bauxite were labelled. The iron content of these samples was then determined in the successive stages of their Bayer processing, using a Ge(Li) semiconductor gamma-spectrometer. In Fig. 11 the gamma-spectrum of the liquor before decomposition is presented. The peak of ^{59}Fe includes both dissolved and suspended iron. After decomposition, this peak cannot be detected in the clear liquor, but appears with high intensity in the hydrate precipitate.

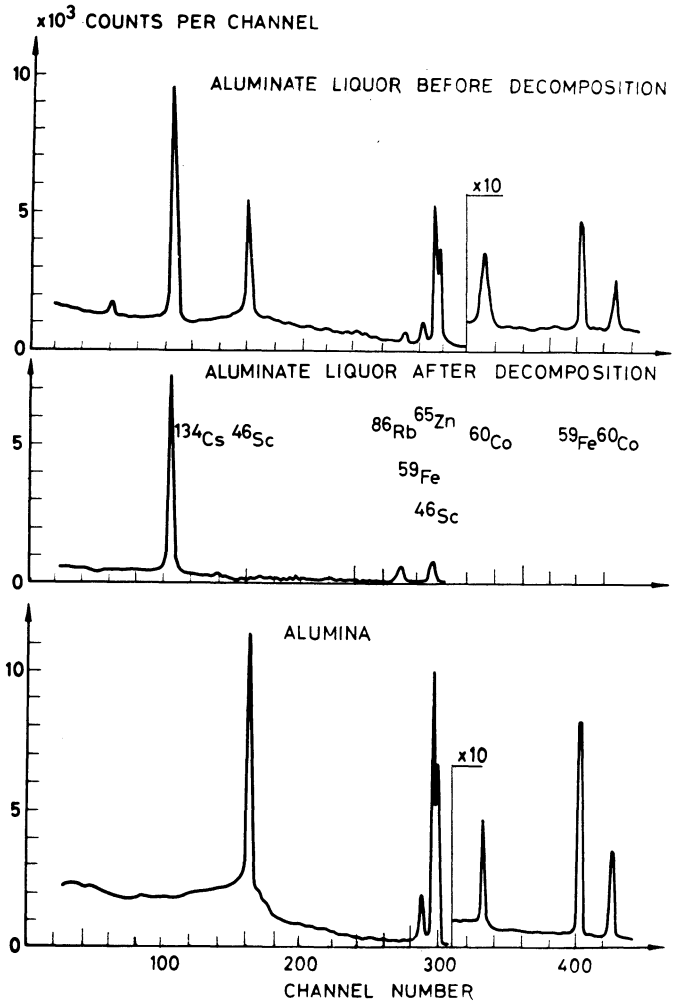

Fig. 11. — γ-ray spectra

We also found that in the case of bauxite samples differing widely in hematite and goethite content, the amount of dissolved, i.e. unfilterable iron is in the range of 2.0 to 3.8 mg Fe_2O_3/litre, practically independent of the mineralogic composition of the bauxite.

The operation of industrial decomposition tanks in series was followed by means of industrial-scale tracer experiments. The objective of these experiments was to determine the mean residence time of the hydrate and the aluminate liquor. By way of example, partial result of an investigation carried out with a decomposition series consisting of 18 tanks with a total volume of 1200 m^3 and agitated by air will be shown. The aluminate liquor was labelled with ^{32}P, the hydrate particles with $^{110\,m}Ag$ precipitated on their surface. The tracers were fed simultaneously to the first tank. To determine residence times, the experiment was continued for almost 40 days and about 1550 samples were measured. The samples were taken from the conduits connecting the tanks. The activity distribution of the hydrate samples leaving the last tank (Fig. 12) shows the recycling of the seed hydrate. The initially sharp maxima become more and more diffuse, as a result of mixing in the decomposition line. From the results of these measurements, the mean age of the seed hydrate can also be determined by representing the results on a logarithmic scale (Fig. 13). A value of 375 hours was found, i.e. a seed hydrate particle dwells in the system

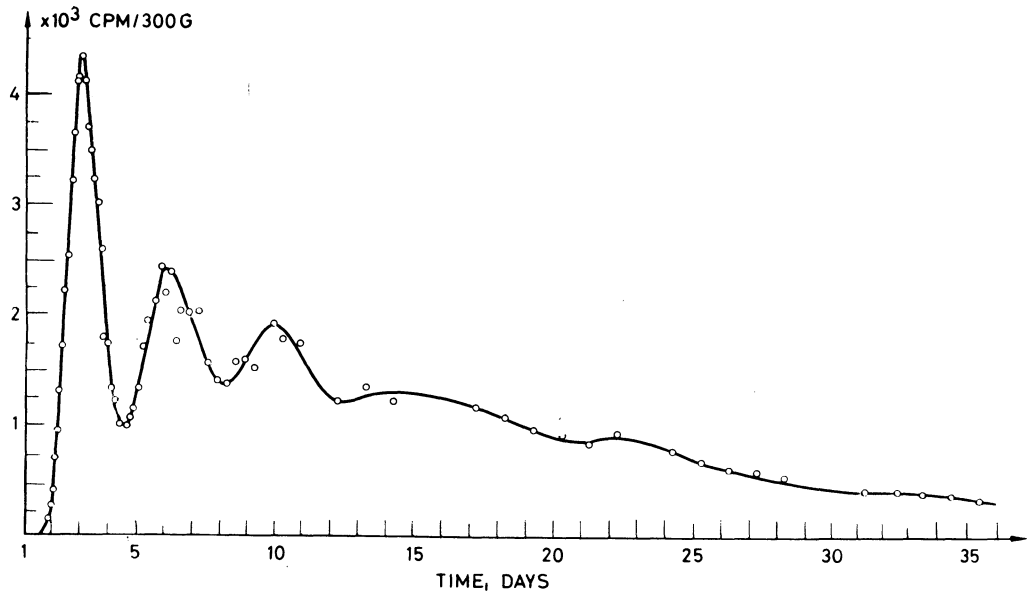

Fig. 12. — Recirculation of hydrate in decomposing tanks in series

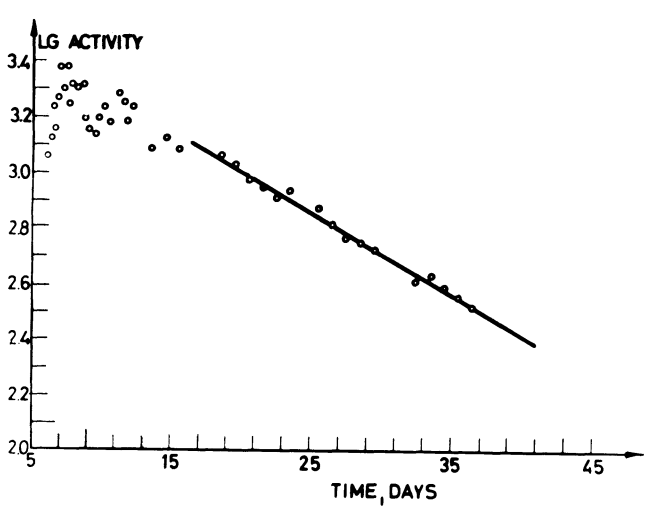

Fig. 13. — Life-time of seed hydrate

for about 16 days on an average. As a result of double tracing we were able to state that by applying intense air agitation, identical residence times of the solid and liquid phases in the decomposition series can be attained.

6. CAUSTICIZATION OF RED MUD

To recover caustic soda losses caused by the formation of sodium-containing compounds in the course of digestion, hydrothermal treatment of red mud with lime or lime hydrate is being applied [35]. The fact that this process has gained relatively little ground, may be attributed to the still uncleared problems in connection with mechanism and optimum conditions of causticization. Our radioisotope tracer studies yielded answers to many questions concerning Na_2O and Al_2O_3 losses and phase transformations in the course of causticization, allowing to draw important conclusions as to the industrial-scale utilizability of the method.

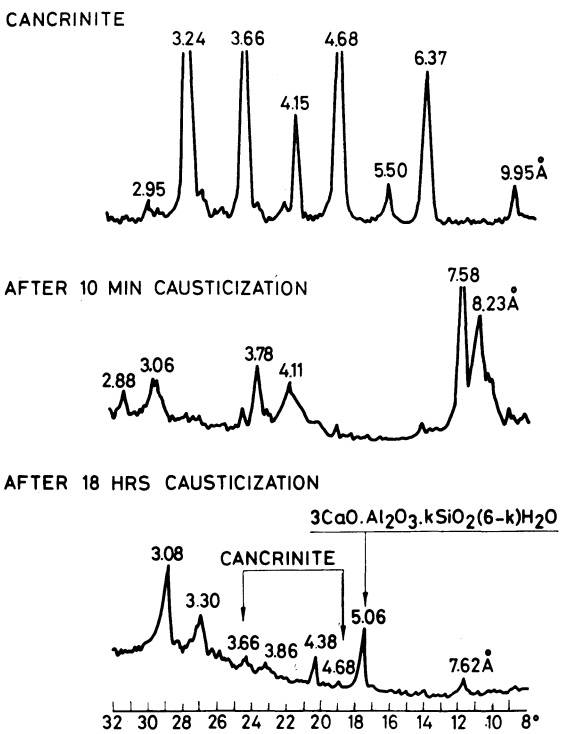

Fig. 14. — X-ray diffractograms

The same pre-treated model substances were used in these studies as described in connection with the wash of red mud. Causticization was carried out in distilled water at 90 °C under the addition of lime in amounts corresponding to the molar ratios CaO: Al_2O_3 = 3 and CaO: TiO_2 = 0.5. Na_2O, Al_2O_3 and SiO_2 concentrations of the solutions were measured and phase transformations were followed by X-ray diffraction studies. The typical lattice structure of sodium aluminium hydrosilicates collapses within a relatively short time at the beginning of causticization. In Fig. 14, the change in the diffraction pattern of cancrinite as a function of the causticization period is shown by way of example. It is a common characteristic of all sodium aluminium hydrosilicates that their conversion proceeds in the direction of calcium aluminium silicate formation.

$$[3CaO \cdot Al_2O_3 \cdot kSiO_2 \cdot (6-k)\ H_2O]$$

through many intermediate phases [19]. Usually, the Al_2O_3 concentration of the solution obtained by causticization is lower by one order of magnitude, that of SiO_2 by two orders of magnitude as compared to the solubility of the model substance. Great differences were detected between the causticizability of sodium aluminium hydrosilicates and sodium titanates (Fig. 15) which cannot be brought into relation with their solubility.

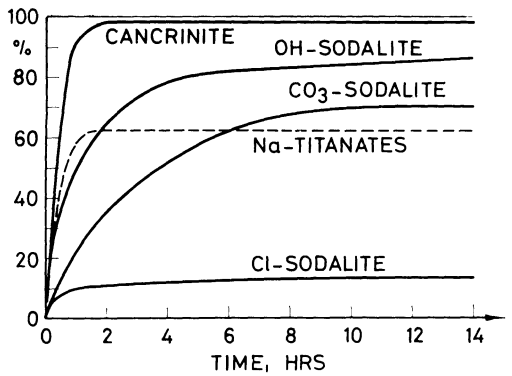

Fig. 15. — Efficiency of causticization

With the discussed examples, we attempted to demonstrate that radioisotope methods have penetrated into the alumina industry both on the laboratory and industrial scale and have contributed to the development in equipment design and to a deeper understanding of the processes.

REFERENCES

[1] SAITO (T.), 1958. — Proc. 2nd Intern. Conf. *P.U.A.E.*, *19*, p. 201.

[2] BUJDOSÓ (E.), IMRE (A.), TÓTH (L.), 1960. — *F.K.I. Közl.*, *4*, p. 65.

[3] BIELFELDT (K.), 1967. — *Aluminium*, *43*, p. 355.

[4] WINKHAUSS (G.), 1972. — Anwendung von Radioisotopen in der Aluminiumindustrie. Informationsheft des Büros Eurisotop, Serie: Monographien, *17*.

[5] BUJDOSÓ (E.), IMRE (A.), TÓTH (L.), 1961. — *Koh. Lapok.*, *94*, p. 66, 114.

[6] BUJDOSÓ (E.), IMRE (A.), TÓTH (L.), 1961. — *F.K.I. Közl.*, *5*, p. 99.

[7] BUJDOSÓ (E.), IMRE (A.), TÓTH (L.), 1963. — *Cvet. Met.*, No. 4, p. 50.

[8] WINKHAUSS (G.), 1968. — V. Int. Leichtmetall-Tagung, Leoben, 1968, *Aluminium-Verlag*, p. 361, Dusseldorf.

[9] WINKHAUSS (G.), 1971. — Proc. 2nd Intern. Symp. I.C.S.O.B.A., *3*, p. 147, Budapest.

[10] BUJDOSÓ (E.), IMRE (A.), TÓTH (L.), 1962. — *Koh. Lapok*, *95*, p. 81.

[11] BUJDOSÓ (E.), MISKEI (M.), 1964. — *Cvet. Met.*, No. 9, p. 64.

[12] BUJDOSÓ (E.), MISKEI (M.), 1964. — *F.K.I. Közl.*, *7*, p. 167.

[13] BUJDOSÓ (E.), MEDWEDEW (W.), MISKEI (M.), 1964. — *Acta Chim. Acad. Sci. Hung. 42*, p. 433.

[14] BUJDOSÓ (E.), MISKEI (M.), ORMOS (Gy.), 1964. — *Koh. Lapok, 97*, p. 419.

[15] BUJDOSÓ (E.), 1967. — Proc. Symp. on Radioisotope Tracers in Industry and Geophys. I.A.E.A., Vienna, p. 409.

[16] BUJDOSÓ (E.), MISKEI (M.), ORMOS (Gy.), 1964. — *Koh. Lapok, 97*, p. 146.

[17] BUJDOSÓ (E.), MISKEI (M.), 1971. — *F.K.I. Közl., 10*, p. 27.

[18] BUJDOSÓ (E.), TÓTH (P.), 1971. — Proc. Res. Inst. Non-Ferrous Metals, *9*, p. 117.

[19] SOLYMÁR (K.), BUJDOSÓ (E.), 1973. — Proc. Sessions 102nd A.I.M.E. Annual Meeting, Chicago (Ill.). *Light Metals, 2*. The Metallurgical Soc. of A.I.M.E. New York, p.717, *T.M.S. Paper* No. A 73-56.

[20] HOLLÓ (L.), LÁSZLÓ (E.), SZEJTLI (I.), LUX (A.), 1965. — *Stärke, 17*, p. 36.

[21] BUJDOSÓ (E.), MISKEI (M.), 1972. — *J. Radioanal. Chem., 11*, p. 99.

[22] LEIPUNSKAYA (D. I.), REZVANOV (R. A.), DRYNKIM (V. I.), 1960. — Yadernaya Geofizika, Gostoptehizdat, Moscow, p. 162.

[23] TATÁR (J.), BÉRESS (M.), 1962. — Proc. Nucl. Geophysicists, Conf. Cracow, *2*, p. 459.

[24] TATÁR (J.), 1964. — *Acta Techn. Acad. Sci. Hung., 47*, p. 455.

[25] DUGAIN (F.), ANDRÉ (M.), 1969. — *C.R.* du Centre de Recherches du Groupe Péchiney.

[26] TATÁR (J.), BÉRESS (M.), SIKLÓS (A.), 1971. — Proc. 2nd Intern. Symp. I.C.S.O.B.A., *3*, p. 23. Budapest.

[27] MISKEI (M.), BUJDOSÓ (E.), 1971. — *F.K.I. Közl., 10*, p. 229.

[28] TAKEUCHI (T.), ISHI (D.), 1964. — Kogyo Kagaku Zasshi, *67*, p. 1835; see CA 62, 1965, p. 9761.

[29] MATULA (M.), 1972. — Magyar Kém. Lapja, *78*, p. 85.

[30] BUJDOSÓ (E.), 1966. — *Koh. Lapok, 99*, p. 567.

[31] RÉNYI (A.), 1959. — M.T.A. Mat. Kut. Int. Közl., *4*, p. 155.

[32] BUJDOSÓ (E.), 1970. — *Acta Phys. Acad. Sci. Hung., 28*, p. 75.

[33] TÓTH (L.). — Unpublished results.

[34] VÓRÓS (I.), BUJDOSÓ (E.), ORBÁN (F.), 1972. — Intern. Colloquium of I.C.S.O.B.A. on Aluminium Production from Low Grade Bauxites, June 6-8, Banska-Bystrica. Czechoslovakia.

[35] VÓRÓS (I.), 1971. — Proc. Res. Inst. Non-Ferrous Metals, *9*, p. 105.

Femkut/ Research Inst. for non-ferrous metals
Fehervari ut 144, 1116 Budapest (Hongrie)